Integrative and Comparative Biology

Integrative and Comparative Biology, volume 61, number 2, pp. 455–463
https://doi.org/10.1093/icb/icab125

Society for Integrative and Comparative Biology

SYMPOSIUM

Regional Patterning in Tail Vertebral Form and Function in Chameleons (*Chamaeleo calyptratus*)

Allison M. Luger [*,1], Peter J. Watson[†], Hugo Dutel[†‡], Michael J. Fagan[†], Luc Van Hoorebeke[§], Anthony Herrel [*,¶] and Dominique Adriaens[*]

[*]Evolutionary Morphology of Vertebrates, Ghent University, 9000 Gent, Belgium; [†]Department of Engineering, University of Hull, HU6 7RX, Hull, UK; [‡]School of Earth Sciences, University of Bristol, BS8 1RJ Bristol, UK; [§]UGCT, Department of Physics and Astronomy, Ghent University, Proeftuinstraat 86/N12, 9000 Gent, Belgium; [¶]UMR 7179 MECADEV, C.N.R.S/M.N.H.N., Département Adaptations du Vivant, Bâtiment d'Anatomie Comparée, 55 rue Buffon, 75005 Paris, France

From the symposium "An Evolutionary Tail: Evo-Devo, Structure, and Function of Post-Anal Appendages" presented at the annual meeting of the Society for Integrative and Comparative Biology virtual annual meeting, January 3–February 28, 2021.

[1]E-mail: Allison.Luger@UGent.be

Synopsis Previous studies have focused on documenting shape variation in the caudal vertebrae in chameleons underlying prehensile tail function. The goal of this study was to test the impact of this variation on tail function using multibody dynamic analysis (MDA). First, observations from dissections and 3D reconstructions generated from contrast-enhanced μCT scans were used to document regional variation in arrangement of the caudal muscles along the antero-posterior axis. Using MDA, we then tested the effect of vertebral shape geometry on biomechanical function. To address this question, four different MDA models were built: those with a distal vertebral shape and with either a distal or proximal musculature, and reciprocally the proximal vertebral shape with either the proximal or distal musculature. For each muscle configuration, we calculated the force required in each muscle group for the muscle force to balance an arbitrary external force applied to the model. The results showed that the models with a distal-type of musculature are the most efficient, regardless of vertebral shape. Our models also showed that the m. ilio-caudalis pars dorsalis is least efficient when combining the proximal vertebral shape and distal musculature, highlighting the importance of the length of the transverse process in combination with the lever-moment arm onto which muscle force is exerted. This initial model inevitably has a number of simplifications and assumptions, however its purpose is not to predict *in vivo* forces, but instead reveals the importance of vertebral shape and muscular arrangement on the total force the tail can generate, thus providing a better understanding of the biomechanical significance of the regional variations on tail grasping performance in chameleons.

Introduction

Chameleons show several adaptations to an arboreal lifestyle, including a fully prehensile tail (Gans 1967). The prehensile tail is a functionally interesting adaptation as it combines a high level of flexibility, enabling the animal to coil its tail around a perch, with the strength needed to suspend the entire body. Regular and substantial mechanical loading of the prehensile tail leads to the expectation that the tail morphology is likely to reflect functional adaptations (Organ 2010). Previous research has focused on the vertebral shape and musculature in an attempt to explain which modifications to the structure confer a functional advantage in grasping, both in chameleons as well as in mammals with prehensile tails. These results have highlighted that prehensile capabilities are a function of the morphology of the musculoskeletal system, both the shape of the caudal vertebrae and the muscular organization (Lemelin 1995; Organ et al. 2009; Organ 2010; Luger et al. 2020). However, most of the previous research investigating prehensile tail morphology has been restricted to descriptions of shape variation: the functional significance of the variation in the musculoskeletal anatomy of the tail for prehension thus remains poorly understood.

Advance Access publication June 10, 2021

The shape of the caudal vertebrae of prehensile-tailed chameleons shows skeletal features likely related to prehensility when compared to those of the largely nonprehensile tails of more terrestrial chameleons (Luger et al. 2020). This study further showed regional variation in vertebral shape within the prehensile tail of chameleons, where the tail can to some degree be divided into a proximal and a distal part. The distal part has a much higher number of smaller vertebrae with shorter vertebral processes (Luger et al. 2020), suggesting a more flexible arrangement than the proximal one, which, in contrast, has more robust vertebrae with a higher width-to-length ratio (Supplementary Fig. S1). Nonprehensile tailed chameleons do not have vertebrae with the typically distal shape but instead have 20–25 caudal vertebrae following the proximal shape pattern. However, the functional significance of this regional variation in the morphology of the tail remains unknown.

The goal of this study was to test the effect of this regional shape variation of the caudal vertebrae on biomechanical function. At this stage, we thus focus only on the effect of vertebral shape variation and variation in the muscular configuration. The architecture of the chameleon tail muscles remains poorly known to date, with previous studies only documenting general aspects of the morphology (Ali 1947; Zippel and Glor 1999; Bergmann et al. 2003). It is therefore currently unknown whether the differences in the shape of the caudal vertebrae between prehensile and nonprehensile tailed chameleon species are associated with differences in the musculature. Also regional differences in vertebrae shape in prehensile-tailed chameleons might be associated with regional variation in the caudal musculature. Variation in the organization and relative size of the muscles between prehensile and nonprehensile-tailed species has been observed in mammals (Lemelin 1995; Organ et al. 2009), with the tail muscles of prehensile-tailed mammals often spanning fewer vertebrae but with relatively larger cross-sectional areas, providing the tail with greater flexibility and strength. The caudal musculature of chameleons has a segmental arrangement, with muscle strands originating on each vertebra and spanning one or more vertebrae before reaching their insertion point. However, the number of vertebrae spanned by each muscle bundle, the precise attachment sites, and whether there is a regional difference within the tail have not been documented. An accurate description of the tail musculature in chameleons is therefore necessary to decipher which aspects of the tail morphology contribute to prehensile function.

Luger et al. (2020) described regional variation in the shape of caudal vertebrae of prehensile-tailed chameleons and suggested that the distinct vertebral morphology in the distal part of the tail enables prehensility. Here, we hypothesize that the regional variation in vertebrae shape is associated with variation in the musculature in prehensile-tailed chameleons. As the distal part of the tail performs a different function compared to the proximal part, namely coiling around and holding onto a perch, we expect this to be reflected in the muscular arrangement. Through testing the effect of musculoskeletal variation on tail function, we also predict that the muscular organization and vertebral shape are optimized in each region for muscle force generation. Consequently, a decrease in the mechanical efficiency of the musculoskeletal system is predicted for deviations from the observed pattern.

To address these questions, we first examined the musculature of the chameleon tail. A combination of dissections and contrast-enhanced μCT scans was used to map the caudal muscular organization and to explore regional variation in the tail musculature. Next, we test the effect of the musculoskeletal variation on the functioning of the tail using multibody dynamic analysis (MDA). MDA is widely used in automotive and aeronautical engineering, as well as biomechanical sciences to study the kinetics of complex systems, for example to model a vertebrate skull or spine mechanics (Curtis et al. 2008; Moazen et al. 2008; Monteiro et al. 2011; Watson et al. 2014; Jones et al. 2017). However, this approach has not been used often to investigate vertebrate tail function (Praet et al. 2012; van Bijlert et al. 2021). Tails are highly complex systems with many connected elements. MDA permits the application of customized forces, as well as constraints, to multiple rigid-bodies, from which output forces or motions can be derived. Through these simulations, the biomechanical parameters such as moments of forces and joint reaction forces during rigid body motion can be calculated. By using imported geometry data, the MDA software also allows the calculation of the center of mass as well as visualizations and accurate simulations of how the musculature is wrapped around the skeletal elements. Together, this makes MDA a suitable method to address our research questions. Creating an accurate MDA model of the entire tail however represents a challenging task. For this preliminary study, therefore only two small sections of the tail are considered, representing the proximal and distal regions. Since no data on muscle activation during gripping are available, we assessed the relative efficiency of each muscle bundle to generate gripping forces while controlling the effect of vertebral shape and muscle attachment location. Since it was not possible to directly predict the gripping forces of the tail, due to the complexity of the modeling, this efficiency was tested as the ability of the muscles to counteract an external force (serving as a proxy for the reaction force generated at a branch when gripping).

Methods

Musculature

Multiple male specimens of *Chamaeleo calyptratus* (Duméril and Bibron 1851) were dissected to study the muscle organization and the origins and insertions of the individual muscle bundles. μCT scans of unstained and phosphomolybdic acid-stained (PMA) samples were made to complement observations made during dissections, allowing us to visualize the soft tissues. The specimens were kept in 2.5% PMA for 2 weeks before scanning, with incisions made in the outer skin layers to facilitate the penetration of the liquids throughout the tissues. All specimens were μCT scanned at the center for X-ray Tomography at Ghent University (UGCT). 2401 projections over 360° were generated. The pixel pitch of the detector was 200 µm (physical detector pixel size) or 400 µm (by binning of four detector pixels) and divided by the sample dependent magnification. The resulting voxel sizes varied between 10 and 85 µm (the higher resolution scans being used needed to visualize the musculature). 3D visualizations of the vertebrae and caudal muscles were generated and digitally segmented in Amira v. 5.5.5 (Visage Imaging, San Diego, CA, USA).

Estimation of maximum muscle forces

The theoretical peak muscle force (F) of each muscle was calculated using the standard equation F = physiological cross-sectional area (PCSA) × muscle stress (S). A range of muscle stress values (25–40 N/cm^2) has been used for calculating muscle force previously (Curtis et al. 2008). We used 30 N/cm^2, following Curtis et al. (2010). To estimate the PCSA we followed Brand et al. (1986), who proposed the equation: PCSA = muscle mass/(density × fiber length). A density of 1.0564 g/cm^3 was used, based on the cat soleus muscle (Murphy and Beardsley 1974). Individual fibers were dissected from two different specimens that were also µCT scanned, in order to obtain the average peak force for each muscle. The m. ilio-caudalis pars ventralis was measured for three different muscles in order to reduce any measurement error as this muscle in particular was difficult to dissect. To obtain the average fiber length for each muscle, 12–43 individual fiber (27 strands on average) from two different individuals were separated per muscle and measured. The thinner the muscle, the more strands were taken to obtain a more accurate estimate, as the chance of breaking was higher than with the thicker muscles. All muscles were removed from the proximal part of the tail. This was impossible for the distal part of the tail due to the small size and tight arrangement of the muscles. To measure the fiber length, muscles were kept in 65% nitric acid for 24 h, after which individual fibers could be removed and their length measured under a microscope.

Multibody dynamic model construction

A multibody dynamic (MDA) model was constructed using the three-dimensional geometries of the vertebrae created from μCT data. Two 3D meshes of the vertebra were used to create our MDA model: one with proximal vertebrae and one with distal vertebrae. Based on the PCA results from Luger et al. (2020), two vertebrae of *C. calyptratus* were chosen that best represented the typical distal and proximal shape. For both vertebral types, six identical vertebrae were created *in silico*, and positioned and aligned using Blender v.2.8, to create a row of articulating vertebrae. Three-dimensional surface models of these were then exported (in .STL file format) and imported to FreeCAD v.0.18.4 to repair errors in the mesh and to convert the meshes into STEP file format for the calculation of inertial properties. These were then imported in ADAMS v2020 (MSC Software Corp., USA) and defined as rigid bodies.

The construction of an MDA model requires the definition of mass properties of the moving bodies, the forces or movements applied to them, and the constraints on these movements. Two randomly chosen proximal and two distal vertebrae were dissected and weighed using an OHAUS Adventurer scale with a sensitivity of 0.001, so that a mass could be assigned to each vertebra in the proximal and distal models respectively. These vertebrae were dissected from the same area of the tail that was replicated by the MDA model. The average weights were 110.8 mg for the proximal vertebrae and 19.5 mg for the distal vertebrae.

Each muscle is segmentally repeated in chameleon tails. The muscles included in both the proximal and distal model were the m. inferocaudalis, the m. longissimus, the m. ilio-caudalis and the m. transversospinalis. Hereafter the two models are referred to as the "proximal vertebrae—proximal musculature" model and "distal vertebrae—distal musculature" model (Fig. 1A and D). The m. ilio-caudalis is divided into a pars dorsalis and a pars ventralis that run separately throughout the tail, divided by the transverse processes, and have different insertion sites. Therefore, they are considered as two separate muscles for this study. The m. inferocaudalis and the m. ilio-caudalis pars ventralis are only present in the proximal region of the tail, and were thus only included in the proximal model—proximal musculature model (Fig. 1A). Each muscle was modelled on both sides of the tail. For muscles with a single origin and insertion site, a single strand was used, running in a straight line from origin to insertion.

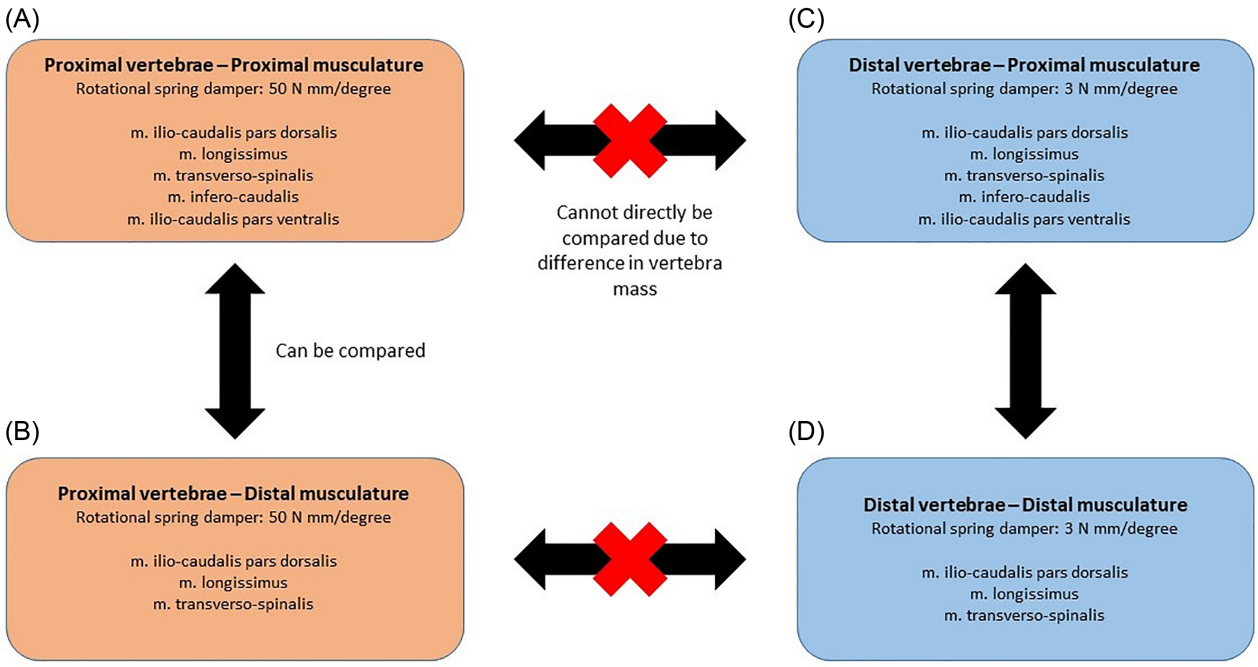

Fig. 1 Overview of the four MDA models used, along with their rotational spring damper and the muscles included in each. It also shows which models could be used for direct comparison and which not.

In case there were two origins or two insertion sites, multiple muscle strands were combined with muscle wrapping (Gröning et al. 2013). When wrapping muscles, they are attached to a cylinder after which a single strand could split into multiple sections, or multiple sections could insert onto the cylinder and continue as a single strand. Such cylinders were placed at the positions at which the muscles split into multiple strands in dissected specimens. The weight of the cylinders was set at 0.1 mg to ensure they weighed significantly less than the vertebrae, thereby minimizing any effect on the movement of the tail.

To ensure kinematic determinacy in both models, a point on the most anterior region of the proximal-most vertebra was constrained in all degrees of freedom, while the separate vertebrae were connected via spherical joints. In an actual specimen, of course the articulation is not only composed of the bony elements, but also of soft, cartilaginous tissue, around which the vertebrae can rotate. Other soft tissues such as ligaments, muscles, and skin further contribute to the movement constraints of the joint. To replicate this in the MDA model a rotational spring damper was added to each spherical joint to restrict the rotation in each axis. As the mass of the proximal vertebrae was over five times larger than that of the distal vertebrae, a different stiffness for the rotational spring was used in the proximal vertebrae—proximal musculature model and distal vertebrae—distal musculature model. The stiffness values were determined as the minimum stiffness required to prevent erratic joint rotations to take place when subjected to a muscle force (2–6 N for each muscle), thus facilitating a smooth and controlled rotation of the tail. Therefore, a stiffness of 3 N mm/deg was defined in the distal vertebrae—distal musculature model, whereas as larger stiffness of 50 N mm/deg was defined in the proximal vertebrae—proximal musculature model. To test the potential influence of the rotational spring damper stiffness on the overall interpretation of the results, sensitivity testing was performed by separately increasing the stiffness by 10% and 20% in both models.

To investigate the mechanical efficiency of the two musculature groups, two further models were created by swopping the musculature acting on each model; these models are referred to as the "proximal vertebrae—distal musculature" and "distal vertebrae—proximal vertebrae." An overview of the research set-up, models and its parameters are given in Fig. 1.

Calculating the total muscle force

To compare the efficiency of the different combinations of vertebral shape and muscular arrangement, in terms of generating muscle force, we calculated the total muscle force required for each muscle type to counteract an external force. We therefore predict that a more optimal muscle arrangement would require less total muscle force to resist the external force and maintain a stationary system at its neutral position. Thus two forces were thus applied to each model: the external force and

the muscle forces from the muscle under consideration. The external force was applied to the distal-most vertebrae of each MDA model. Depending on which muscle was activated, the external force was positioned in an opposite direction to which the tail would be rotating, thus working directly against the total muscle force. Muscles associated with ventral bending are the m. ilio-caudalis pars dorsalis, the m. inferocaudalis and the m. ilio-caudalis pars ventralis. The m. transverso-spinalis is associated with dorsal bending, while the m. longissimus generates lateral bending. For the latter, the total muscle force was calculated with only the left side activated. Multiple simulations were run for each of the four separate models (Fig. 1) through initially varying the external force from 2 to 3, 4, 5, and 6 N (higher forces caused the models to become unstable). For each external force, a single muscle was activated and the force in the muscles incrementally increased by 0.1 N until the total force in that muscle (summation of forces in each strand) was sufficient to counter the external force and revert the tail back to the neutral position. This was repeated for all muscles in the model, thus calculating the force required in each muscle to balance the defined external force.

Results

The caudal musculature and theoretical peak muscle forces

The musculature of *C. calyptratus* differed between the proximal and distal part of the tail. Only three muscles ran through the entirety of the tail, namely the m. ilio-caudalis pars dorsalis, the m. longissimus and the m. transverso-spinalis. The m. ilio-caudalis pars ventralis and the m. infero-caudalis only run along the proximal part of the tail. An overview of the musculature is given in Supplementary Figs. S2 and S3.

For the description of the musculature, the first vertebra from which the muscle originates is referred to as "V1," the subsequent vertebra as "V2," etc. Each muscle runs both on the left and right side of the vertebrae. For the proximal musculature, the m. transverso-spinalis originates at the top of the neural spine on V1 (Supplementary Fig. S2). Approximately after crossing V2, it splits and inserts on two sites: one on the vertebral body of V4 near the base of the neural spine and one at the tip of the postzygapophysial process on V5. The m. longissumus originates at two different sites on V1, both at the tip of the prezygapophysial process and on the tip of the haemal arch. The m. longissimus bundles join around V4, after which they continue as a single bundle inserting at the base of the transverse process on V5. The m. ilio-caudalis pars dorsalis does not split but originates at the tip of the transverse process on V1 and runs in a straight line to its insertion at the base of the transverse process of V5. The m. ilio-caudalis pars ventralis also originates near the tip of the transverse process of V1 but ventral to that of the m. ilio-caudalis pars dorsalis. It splits around V3 into two bundles both inserting on V6, one at the tip of the chevron bone and one at the tip of the transverse process. The m. infero-caudalis runs ventrally, inserting on the distal tip of each chevron bone. It forms a continuous muscle strip up to the V25–27, but with an insertion on each vertebra.

The distal region of the tail only has three muscles. The m. transverso-spinalis originates at the tip of the neural spine of V1 but does not split in two bundles as it does in the proximal region. It runs in a straight line and inserts at the base of the neural spine of V5. The m. longissimus is more similar in both the proximal and distal regions. It has two origin sites on V1, one at the tip of the prezygapophysial process and one near the ventral side of the vertebral body (as chevron bones are absent here). The two bundles merge around V3 and insert dorsally on the body of V6, thus one vertebra further than it does in the proximal region. The m. ilio-caudalis pars dorsalis crosses fewer vertebrae in the distal region than it does proximally, as it originates on the tip of the transverse process of V1 and runs in a single bundle inserting again at the base of the transverse process on V3. The calculated theoretical muscle peak force range between 0.7 and 5 N for all muscles (Supplementary Table S1).

Mechanical efficiency of musculature

The results of the MDA are presented in Fig. 2. Due to the acute insertion angle of m. ilio-caudalis pars ventralis in the distal vertebrae—proximal musculature model (Supplementary Fig. S2), the activation of the muscle produced excessive movement, which rendered the simulations unstable. Therefore, this model was left out of the analysis of the distal vertebrae—proximal musculature model.

The simulations show that the models powered by the proximal musculature require a higher total muscle force in order to counteract the external force, when compared with the distal musculature (Fig. 2). Regardless of the combination of vertebral shape and musculature, the total muscle force for each muscle increased linearly with increasing external force ($R^2 > 0.925$). The m. transverso-spinalis in each model, and the m. ilio-caudalis pars dorsalis in the distal vertebrae—proximal musculature model, had a steeper slope in Fig. 2 compared to the other muscles. With an increasing external force, relatively higher total muscle forces are needed here to stabilize the model at the neutral position. For the m. ilio-caudalis pars dorsalis in the

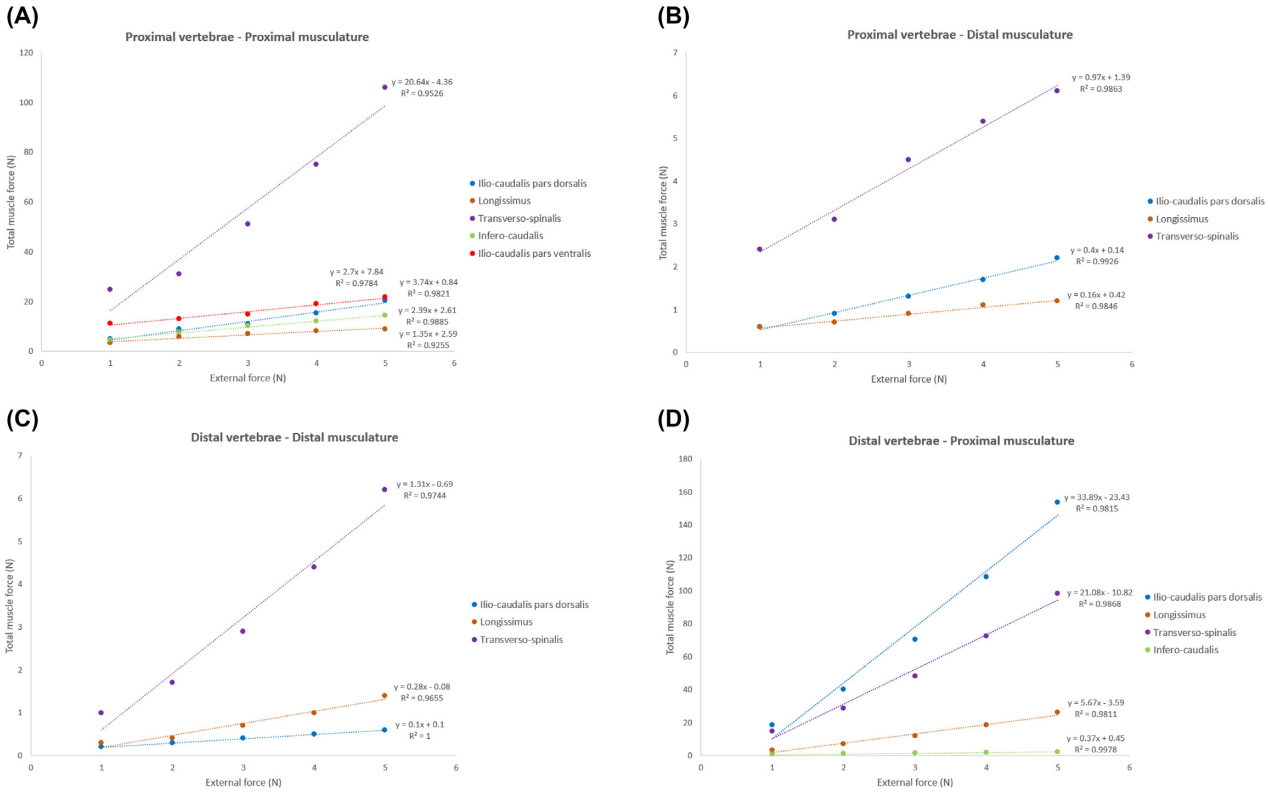

Fig. 2 Graphs showing the muscle force needed to counteract the external force. Linear regressions with R^2 values are provided for each muscle: (**A**) simulations of the proximal vertebrae—proximal musculature model; (**B**) simulations of the proximal vertebrae—distal musculature model; (**C**) simulations of the distal vertebrae—distal musculature model; and (**D**) simulations of the distal vertebrae—proximal musculature model.

distal vertebrae—proximal musculature model this rises to 160 N, while for the distal vertebrae—distal musculature model this is only 0.6 N.

When comparing the total muscle force values between models with the same vertebrae, a large difference can be observed. For example, for the proximal vertebrae—distal musculature a total muscle force of only up to 6 N is needed for the m. transverso-spinalis, and is even less (<3) for the other muscles (Fig. 2B). However, in the proximal vertebrae—proximal musculature model, the m. transverso-spinalis needs more than 100 N to reach this stability (for the other muscles this is 22 N and lower) (Fig. 2A). Similarly, the distal vertebrae—distal musculature model needed a relatively lower total muscle force to stabilize the model, the highest being 6 N for the m. transverso-spinalis (Fig. 2C). In comparison, the proximal musculature—distal vertebrae model needed between 26 and 153 N to counter the external force, with the exception of the m. infero-caudalis that only required 2.3 N (Fig. 2D). The results of the sensitivity are provided in the Supplementary data (Supplementary Fig. S4). For each model the results showed an R^2 value greater than 0.9, which are in line with the results depicted in Fig. 2, meaning that the change in rotational spring damper does not affect the muscle forces too much and thus the conclusions stay the same.

Discussion

The dissections and μCT data allowed us to observe regional difference in the caudal musculature of *C. calyptratus*. Our observations showed that there is a regional variation within the musculature, reflecting that found in the skeletal morphology, distinguishing a typical proximal and distal arrangement (Luger et al. 2020). Using MDA, we could show that the regional differences in vertebral shape and muscle arrangement have an impact on the mechanical efficiency of the musculoskeletal system. It is important to note that these musculoskeletal models do not take account of the effects of physiological and other parameters that define *in vivo* musculo-skeletal performance, and thus entail several simplifications. For example, the constraints imposed by the soft tissue on vertebral movement are not based on measured values, but instead an arbitrary chosen rotational spring damper was applied to allow the tail to move in a smooth and controlled manner. Moreover, values such as muscle mass and pennation angle were

not considered, which can have an effect on the muscle force output (Curtis et al. 2010). Even at the level of vertebral shape, this variation was simplified by only comparing the shape of an average proximal vertebra with an average distal vertebra, thereby omitting the existing serial variation within each vertebral region. Yet, despite these simplifications, the results show that the regional differences in vertebral shape and muscle arrangement affect the mechanical efficiency of the tail muscles.

Regarding the musculature, it is not as straightforward to assume that the predictions calculated from our models could directly be directly translated to other squamates. While few descriptions of the caudal musculature exist in squamates, Zippel and Glor (1999) previously compared the caudal musculature of the chameleon *Furcifer* with the skink *Corucia* and showed that these have a very different anatomical organization. This organization found in *Corucia* is thought to closely match that as found in other species capable of caudal autotomy, where the musculature forms "cones" corresponding to each segment. This drastically different anatomical organization makes it difficult to compare both systems, though it would be interesting to include such species in future research.

The models with the distal musculature require less total muscle force (Fig. 2B and C) than those with the proximal musculature (Fig. 2A and D) to counteract an external force of the same magnitude. This suggests that the distal musculature is more efficiently arranged with respect to the distal vertebrae in terms of mechanical advantage. This is consistent for all distal muscles explored, that is, the m. ilio-caudalis pars dorsalis, the m. longissimus, and the m. transverso-spinalis. For the distal musculature, the simulations showed that relatively low total muscle forces (6 N or less) were needed to counteract the largest external force. For the proximal musculature, a total muscle force of 20 N or higher was common, with some being much higher such as the m. transverso-spinalis reaching values above 100 N.

The m. ilio-caudalis pars dorsalis for the distal vertebrae—proximal musculature model requires a far higher total muscle force to withstand the external forces, on average five times higher than for the other models where it is a highly efficient muscle. At the level of the proximal vertebrae it spans more vertebrae than it does distally. Proximally, it also attaches to longer transverse processes, and therefore has a longer lever arm acting onto the intervertebral joints. The resulting longer muscle moment arm enables the muscle to generate a higher moment, which is substantially constrained at the distal vertebrae due to the small transverse processes. The other muscles that attach to the transverse processes have multiple insertion sites, rather than the single insertion site of the m. ilio-caudalis pars dorsalis, and as such have an increased lever arm. This muscle is also much shorter in its distal arrangement, inserting on V3 instead of V5 proximally. The relatively shorter muscle increases the angle along which the force is being directed, allowing it to generate a higher moment. The longer muscles and shorter transverse processes makes this proximal muscle organization acting upon distal vertebrae a highly inefficient system. It can thus be concluded that this muscle organization matches the vertebral shape for improved bending performance. The importance of a long transverse process for ventral tail bending is congruent with the conclusions of previous studies (Youlatos 2003; Organ et al. 2009; Luger et al. 2020).

The m. ilio-caudalis pars dorsalis (which moves the tail downwards) requires less total muscle force to counteract the external forces than the m. transverso-spinalis (which moves the tail upwards). Except for the set-up with the distal vertebrae and proximal musculature, these results are observed in the other three models. For these models, the m. transverso-spinalis requires on average 4.7 times as much muscle force than the m. ilio-caudalis pars dorsalis. The higher efficiency of the m. ilio-caudalis pars dorsalis may explain how the tail can grab well when moving the tail downwards as is required for a grabbing motion. This muscle would be more important for prehension, especially when compared to the m. transverso-spinalis.

In the proximal part of the tail, two additional muscles assist in bending the tail downward: the m. infero-caudalis and the m. ilio-caudalis pars ventralis. Although the models with a proximal musculature show on average a higher total muscle force than the models with the distal musculature, the m. infero-caudalis has relatively low values, reaching up to 2.3 N with the distal vertebrae set-up. The larger size of the proximal part of the tail allows room for all three muscles and by activating a combination of these synchronously, the proximal musculature should still be able to generate a higher combined total muscle force in the ventral direction. As no data on muscle activation patterns are available it is for now impossible to determine the relative contribution of each muscle during gripping and coiling. Comparing the m. longissimus with the other muscles is also complicated. As only one-half of the muscles were activated at one time it cannot be compared directly to the other muscle groups; moreover, its values would need to be doubled. The m. longissimus requires a relatively low total muscle force in each set-up. Lateral rotation is important for coiling the tail, together with ventral flexion, and both movements are needed for prehensile function (Lemelin 1995; Organ et al. 2009). As this is the only muscle responsible for lateral movement throughout the tail, it is expected that its arrangement

maximizes its efficiency both for the proximal and distal musculature.

The m. transverso-spinalis requires a relatively high total muscle force to stabilize the model at its neutral position. In most models, the m. transverso-spinalis in Fig. 2 has a greater slope than the other muscles, suggesting it is less efficient compared to these muscles, the exception being the set-up with the distal vertebrae and proximal musculature in which the m. ilio-caudalis pars dorsalis has a greater slope in Fig. 2. With the proximal musculature, regardless of whether it is in combination with the proximal or distal vertebrae, the m. transverso-spinalis requires more than 100 N to stabilize the model. This indicates that vertebral shape is not the major influence on the efficiency on this muscle. The proximal part of the tail has very little dorsal flexibility and this muscle would only be used in this region to stabilize the tail when walking, which is reflected in the low efficiency of this muscle to generate force (Zippel and Glor 1999). Dorsal bending of the tail is required during the release of the tail and the aiming for a branch to grasp onto, as well as for maintaining tail posture and keeping the tail from dragging on the substrate during locomotion. The muscles responsible for these movements thus likely do not have the same demands to generate a high force compared to when coiling the tail around a perch and withstanding an animals' entire body weight. The other muscles are likely to play a more important role in tail prehension and are able to attain the same results with a lower total muscle force, which is reflected in the results in terms of efficiency.

The output of the theoretical muscle force showed that the caudal muscles are able to generate maximum forces between 0.7 N for the lowest (m. transverso-spinalis) and 4.9 N for the highest muscle force (m. ilio-caudalis pars dorsalis). The results from the models using the distal musculature are in line with the theoretical muscle force, those using the proximal musculature are often much higher. This again could indicate that the proximal musculature is less optimized for muscle force generation as the muscles are anatomically capable of generating much higher forces when arranged in a more optimal configuration.

The results of the sensitivity test showed that the values of the rotational spring damper did not have a marked influence on the results. Since this is a comparative study between the results of the different models, rather than prediction of an absolute muscle force, our chosen rotational spring damper values have proven to be adequate for this study. One of the disadvantages of the current method of calculating the total muscle force to balance against an external force is that it represents a single static situation. As such, the current model does not account for a changing geometries and changing muscle moment arms as the model moves during muscle activation. Future models should incorporate this so that prehensile performance in relation to range of motion can be mapped, which would require more accurate *in vivo* and EMG data. The latter would allow the integration of muscle activation patterns into the model. The models applied in this study only activate individual muscles separately, thereby moving the model in a single direction. However, actual tail movement will be a complex but organized interaction of antagonistic and agonistic muscles. Another improvement to the current model that could be considered, is to measure the joint stiffness resulting from the surrounding soft tissue, as well as the range of motion defined by the vertebral articulations (both body and zygapophysial articulations). This would allow quantification of the rotational spring damper, and thus allow more accurate comparisons between the models with the proximal and distal vertebral shape. In the current model this was not possible, as the rotational spring damper would influence the total muscle force needed to stabilize the model at its initial resting position. To further complete the model, other parameters like bone density, pennation angle, and mass of individual vertebrae would have to be included. For the PCSA, we made the assumption that the pennation angle is zero, as the evaluation of such is not within the scope of this research, however this could be included for future research. That MDA models are sensitive to proper parameter inclusion and quantification was shown by Gröning et al. (2013) who compared the predicted bite forces of a lizard skull using MDA models, with those measured *in vivo*. They found that, while the results of their model came close to the *in vivo* measurements, the model was very sensitive to changes in muscle properties. Changing parameters such as fiber lengths, muscle stress, pennation angle, and force orientation lead to different bite force predictions, emphasizing the necessity of having accurate muscle measurements when building realistic MDA models. Both Curtis et al. (2008) and Gröning et al. (2013) also showed the importance of accurate muscle wrapping by showing how changing the representations of the muscles influences the muscle force output. While our model currently only includes vertebral shape variation and variation between the insertion and origin sites of the caudal musculature, for future research it would be interesting to include such parameters. The muscle size and volume, as well as the muscle physiology, while beyond the scope of this current paper, would allow us to make more accurate predictions approximating the *in vivo* data.

Despite the limitations in the current model, the simulations showed that overall shape and musculature differences between proximal and distal vertebrae have

a large influence on the outcome of the simulated mechanical performance. This study presents one of the first attempts to understand tail function using MDA and the results show that this is a promising method to explore the evolution of tail prehensile capabilities in different vertebrates, and could be transferred to more complex systems with multiple connected rigid bodies. Previous work done on seahorses by Praet et al. (2012) did include an MDA model on a seahorse prehensile tail, which was comprised a less complex system (both at the level of muscle architecture as at the level of vertebral shape variation) than the current model. We approximate a higher level of anatomical realism in the current model. This study also presents an accurate overview of the muscular architecture of the caudal muscles including the theoretical muscle forces.

Acknowledgments

The authors would like to thank Iván Josipovic and Matthieu Boone from the UGCT; Jens De Meyer, Aurélien Lowie, Pasha van Bijlert, and Robert Paauwe for their feedback; Barbara De Kegel for her assistance with the lab work; and Alexis Dollion for providing us with the chameleons. We would also like to thank Katrina Jones and the two anonymous reviewers for their constructive reviews, as well as Suzanne Miller for being a considerate editor.

Funding

This work was supported by the Fonds Wetenschappelijk Onderzoek [#3G006716] and a Tournesol mobility grant.

Supplementary data

Supplementary data available at *ICB* online.

Data availability

Data available upon request.

References

Ali SM. 1947. Studies on the anatomy of the tail in Sauria and Rhynchocephalia II. *Chameleon zeylanicus* Laurenti. Proc Indian Acad Sci 28:151–65.

Bergmann PJ, Lessard S, Russell AP. 2003. Tail growth in *Chamaeleo dilepsis* (Sauria: Chamaeleonidae): functional implications of segmental patterns. J Zool 261:417–25.

Brand RA, Pedersen DR, Friederich JA. 1986 The sensitivity of muscle force predictions to changes in physiological cross-sectional area. J Biomech 19:589–96.

Curtis N, Jones MEH, Lappin AK, O'Higgins P, Evans SE, Fagan MJ. 2010. Comparison between in vivo and theoretical bite performance: using multi-body modelling to predict muscle and bite forces in a reptile skull. J Biomech 43: 2804–9.

Curtis N, Kupczik K, O'Higgins P, Moazen M, Magan MJ. 2008. Predicting skull loading: applying multibody dynamics analysis to a macaque skull. Anat Rec 291:491–501.

Duméril AMC, Duméril AHA. 1851. Catalogue méthodique de la collection des reptiles du Muséum d'Histoire Naturelle de Paris. Gide et Baudry/ Roret Paris:224.

Gans C. 1967. The chameleon. Nat Hist 76:52–9.

Gröning F, Jones MEH, Curtis N, Herrel A, O'Higgins P, Evans SE, Fagan MJ. 2013. The importance of accurate muscle modelling for biomechanical analyses: a case study with a lizard skull. J R Soc Interface 10:20130216.

Jones MEH, Gröning F, Dutel H, Sharp A, Fagan MJ, Evans SE. 2017. The biomechanical role of the chondrocranium and sutures in a lizard cranium. J R Soc Interface 14: 20170637.

Lemelin P. 1995. Comparative and functional myology of the prehensile tail in new world monkeys. J Morphol 224: 351–68.

Luger AM, Ollevier A, De Kegel B, Herrel A, Adriaens D. 2020. Is variation in tail vertebral morphology linked to habitat use in chameleons. J Morphol 281:229–39.

Moazen M, Curtis N, Evans SE, O'Higgins P, Fagan MJ. 2008. Combined finite element and multibody dynamics analysis of biting in a *Uromastyx hardwickii* lizard skull. J Anat 213:499–508.

Monteiro NMB, da Silva MPT, Folgado JOMG, Melancia JPL. 2011. Structural analysis of the intervertebral discs adjacent to an interbody fusion using multibody dynamics and finite element cosimulation. Multibody Syst Dyn 25: 245–70.

Murphy RA, Beardsley AC. 1974. Mechanical properties of the cat soleus muscle in situ. Am J Physiol 227:1008–13.

Organ JM, Teaford MF, Taylor AB. 2009. Functional correlates of fiber architecture of the lateral caudal musculature in the prehensile and nonprehensile tails of the Platyrrhini (Primates) and Procyonidae (Carnivora). Anat Rec 292: 827–41.

Organ JM. 2010. Structure and function of Platyrrhine caudal vertebrae. Anat Rec 293:730–45.

Praet T, Adriaens D, Van Cauter S, Masschaele B, De Beule M, Verhegghe B. 2012. Inspiration from nature: dynamic modelling of the musculoskeletal structure of the seahorse tail. Int J Numer Methods Biomed Eng 28:1028–42.

van Bijlert PA, van Soest AJK, Schulp AS. 2021. Natural Frequency Method: estimating the preferred walking speed of Tyrannosaurus rex based on tail natural frequency. R Soc Open Sci 8:201441.

Watson PJ, Gröning F, Curtis N, Fitton LC, Herrel A, McCormack SW, Fagan MJ. 2014. Masticatory biomechanics in the rabbit: a multi-body dynamics analysis. J R Soc Interface 11:20140564.

Youlatos D. 2003. Osteological correlates of tail prehensility in carnivorans. J Zool 259:423–30.

Zippel KC, Glor RE. 1999. On caudal prehensility and phylogenetic constraint in lizards: the influence of ancestral anatomy on function in *Corucia* and *Furcifer*. J Morphol 239:143–15.